Available online at http://scik.org

Commun. Math. Biol. Neurosci. 2026, 2026:42

https://doi.org/10.28919/cmbn/9668

ISSN: 2052-2541

ANALYTICAL AND NUMERICAL INVESTIGATION OF INFLUENZA TRANSMISSION WITH VACCINATION AND TREATMENT: STABILITY, SENSITIVITY AND BIFURCATION PERSPECTIVE

DIPAK MAJI[1], NAV KUMAR MAHATO[1], ADITYA GHOSH[2,*]

[1]Department of Mathematical Sciences, School of Basic and Applied Sciences, Adamas University, Kolkata, India

[2]Department of Mathematics, Amity Institute of Applied Sciences, Amity University, Kolkata, India

Abstract: The impact of parameters on influenza dynamics deeper insights to understand and control the spread of the disease. The present study examines the impact of parameters on the transmission dynamics of the influenza virus through a nonlinear SVITR (Susceptible–Vaccinated–Infected–Treated–Recovered) model. The Basic Reproduction Number R_0 is studied using Next Generation Metrix. Furthermore, the model exhibits transcritical bifurcation, where stability shifts between equilibria as critical parameter thresholds, particularly the transmission rate, are crossed. Numerical simulations validate the theoretical results, demonstrating the sensitivity of disease dynamics to variations in the model and identifying key parameters that significantly influence disease spread. Based on different parameter values, stability analysis is performed for disease-free and endemic equilibria. The model's positivity, boundedness, and uniqueness are also established to ensure biological feasibility. These findings offer valuable insights for designing effective control strategies against influenza outbreaks.

Keywords: modelling; influenza; stability analysis; basic reproduction number; bifurcation.

2020 AMS Subject Classification: 92D30.

*Corresponding author

E-mail address: ghosh.aditya.iitg08@gmail.com

Received Oct. 28, 2025

1. INTRODUCTION

Influenza is a globally prevalent acute respiratory infection that remains a substantial threat to public health due to its seasonal recurrence, capacity for mutation, and pandemic potential. Each year, it infects an estimated 3–5 million people globally and results in 250,000 to 500,000 deaths, as reported by the World Health Organization [1]. Historical pandemics, such as the 1918 Spanish flu, the 1957 Asian flu, and the 1968 Hong Kong flu, collectively caused tens of millions of fatalities, highlighting the persistent danger posed by influenza viruses [1]. In the Indian context, major outbreaks such as the 2014–2015 H1N1 epidemic and the 2024 detection of avian influenza A (H9N2) reaffirm the national burden of this disease [2].

Transmission occurs primarily via respiratory droplets and direct or indirect contact with contaminated surfaces, leading to symptoms like fever, cough, and fatigue [3,4]. Antigenic drift and shift [5], which allow the virus to evade immune responses, further complicate vaccine development and effectiveness. The global circulation of diverse influenza virus subtypes, as observed in WHO surveillance data from 2011 to 2023, has revealed notable spatiotemporal variations in epidemic timing and strain dominance, underscoring the need for adaptive public health strategies [1]. The COVID-19 pandemic has altered influenza transmission patterns by changing travel behaviours, social contact rates, and healthcare system focus, thus revealing complex inter-virus ecological dynamics [6].

Over the past two decades, mathematical modeling has emerged as a vital tool for understanding and predicting the transmission dynamics of influenza and other infectious diseases. Classical compartmental models such as SIR, SEIR, and their extensions have laid the foundation for epidemic forecasting and policy evaluation [7,8]. Hethcote [7] provides a detailed overview of mathematical formulations in epidemiology, while Earn et al. [6] discuss the ecological and evolutionary dynamics of influenza viruses. Advanced models have incorporated complex features, such as partial immunity [9], adaptive immunity [10], seasonality [11], and age structure [12], enhancing the biological realism and predictive power of model outcomes.

Several studies have focused on control strategies using optimal intervention models. Srivastav and Ghosh [4] analyzed optimal control in a basic influenza model, and Lee et al. [12] incorporated seasonal and age-specific factors. Kanyiri et al. [13] modelled drug resistance dynamics in influenza A, while Hussain et al. [14] explored swine influenza control using an optimal control framework. Additionally, atomic-level modelling has revealed protein-structure vulnerabilities that may inform antiviral development [15].

Despite widespread vaccination campaigns, limited efficacy and rapid viral evolution necessitate supplementary strategies such as antiviral treatments and behavioural interventions [16,17]. Treatment not only reduces symptom severity and viral shedding duration but also mitigates secondary transmission, particularly in high-risk groups [15]. The interplay between vaccine coverage, treatment uptake, and natural immunity dynamics requires a multi-parameter analytical approach to guide intervention policy.

Furthermore, the complex interactions between multiple respiratory viruses such as influenza and SARS-CoV-2 have recently gained attention, particularly in the context of co-infection. Maji and Ghosh [18] developed a mathematical framework to study the dual dynamics of these viruses, emphasizing the influence of parameter variations on their co-spread and control measures. This motivates the need to analyze such models in greater detail.

In this study, we develop a nonlinear SVITR (Susceptible–Vaccinated–Infected–Treated–Recovered) model to capture key mechanisms of influenza transmission, including vaccination, treatment, and reinfection. The model is analyzed using a combination of theoretical and numerical methods. The basic reproduction number is derived via the next-generation matrix approach [19,20], and a normalized forward sensitivity analysis identifies key parameters influencing [21] and global stability [22] of the model. Furthermore, we establish the occurrence of a transcritical bifurcation [23,24], demonstrating how a shift in transmission rate can destabilize the disease-free equilibrium and lead to the persistence of infection. This behaviour is analysed using the Center Manifold Theorem.

Numerical simulations validate the analytical findings and show how parameter variations influence infection burden. The results align with prior influenza modelling work [24–26], providing actionable insights into the design of more effective, data-driven intervention strategies. In summary, this work contributes to the growing body of literature on infectious disease modelling by offering a robust SVITR framework that incorporates core influenza dynamics. It advances the understanding of disease control thresholds, parameter sensitivities, and bifurcation structures and can be extended to model complex phenomena such as co-infections, antiviral resistance, and strain evolution.

2. MODEL FORMULATION:

To investigate the transmission dynamics of influenza, we develop a nonlinear compartmental model by dividing the total human population $N(t)$ into five distinct groups namely $S(t)$ be the susceptible individuals any at time t. $V(t)$ be vaccinated individuals at time t. $I(t)$ be the infected individuals at time t and $T(t)$ be the individual that receiving treatment and $R(t)$be the recovered individuals at any time t .Here we assume that the individual enters the population at a constant recruitment rate π and all such populations are assumed to be susceptible. The susceptible individuals become infected after effective contact with the infected or treated individuals, at a transmission rate β.Treated individuals have reduced infectiousness, captured by factor $\varepsilon \in [0\ 1]$ Suspectable individual are vaccinated at a rate ϕ.However the vaccinated individual is not fully protected or may still acquire infection depending on the vaccination efficacy ε.Th e infected individual begin treatment at rate ξ and recovers from treatment at a rate α, or dies due to disease at a rate δ .The recovered individual loses the immunity and returns to the susceptible class at a rate of γ.all component are subject to the natural death rate μ .

Based on the following assumption, the model is governed by the following nonlinear equation

$$\frac{dS}{dt} = \pi + \gamma R - \beta SI - \phi S - \mu S$$

$$\frac{dV}{dt} = \phi S - (1-\varepsilon)\beta VI - \mu V$$

$$\frac{dI}{dt} = \beta SI + (1-\varepsilon)\beta VI - (\mu + \xi + \gamma + \delta)I \quad (1)$$

$$\frac{dT}{dt} = \xi I - (\mu + \alpha)T$$

$$\frac{dR}{dt} = \alpha T + \gamma I - (\mu + \gamma)R$$

Table1: The details of the parameters

Symbol	Description
π	Recruitment rate new individuals entering the population (e.g., birth or immigration)
β	Transmission rate at which susceptible individuals become infected upon contact with infected individuals
ε	Vaccination efficiency Reduction factor for vaccinated individuals getting infected $0 \leq \varepsilon \leq 1$
μ	Natural Death rate (applied for all compartment)
ϕ	The rate at which a susceptible proportion of the human population is Vaccinated
γ	Recovery rate/Immunity loss rate
δ	Disease-induced death rate
α	Recovery rate of the treated population
ξ	Rate at which infected individuals start treatment (Treatment rate)

2.3. MODEL DIAGRAM:

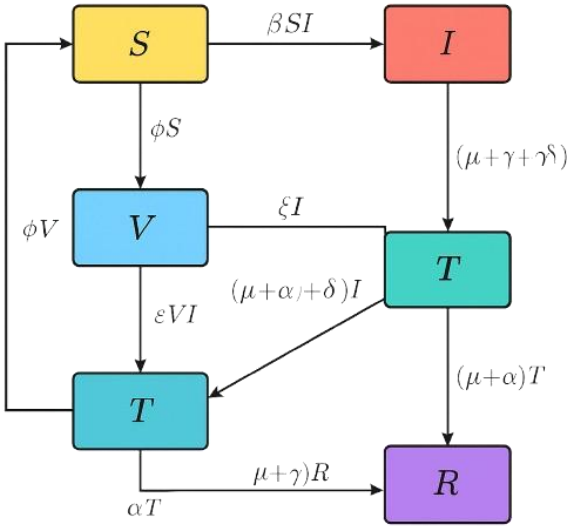

Figure 1: Model Diagram

3. MODEL ANALYSIS

3.1 BASIC PROPERTIES

3.1.1 POSITIVITY OF THE SOLUTIONS:

The dynamical system described by equation (1) governs the temporal evolution of various human population compartments. To ensure the model's biological feasibility, it is essential to demonstrate that the solutions remain non-negative for all future time $t > 0$, provided the initial conditions are non-negative. This property is formally established in the following theorem.

Theorem 3.1. Let $S(t) \geq 0$, $I(t) \geq 0, V(t) \geq 0, T(t) \geq 0$ *and* $R(t) \geq 0$ denote the initial condition of the STVIR model. Then, the solutions $S(t), I(t), V(t), T(t), R(t)$ are non-negative for all $t \geq 0$

Proof: We prove the non-negativity of each state variable by analyzing the structure of the differential equations and applying the comparison principle.

Consider the equation for the susceptible population;

$$\frac{dS}{dt} = \pi + \gamma R - \beta SI - \phi S - \mu S$$

$$\frac{dS}{dt} = \pi + \gamma R - (\beta I + \phi + \mu)S$$

Noting that $R(t), I(t), S(t) \geq 0$ and all parameters are non-negative, we obtain:

$$\frac{dS}{dt} \geq \pi + \gamma R \qquad (2)$$

Now at the boundary $S = 0$ and $R \geq 0$, $I \geq 0$.

$$\left(\frac{dS}{dt}\right)_{S=0} \geq \pi + \gamma R$$

Hence $S(t)$ can not cross the plane $S = 0$ into negative values, and $S(t) \geq 0$ for all $t \geq 0$

For vaccination compartment:

$$\frac{dV}{dt} = \phi S - (1 - \varepsilon)\beta VI - \mu V$$

At $V = 0$

$$\left(\frac{dV}{dt}\right)_{V=0} \geq \phi S$$

Since the right-hand side is linear in $V$and $\phi S \geq 0$,it follows that $V(t) \geq 0$ for all $t \geq 0$,

Provided $V(t) \geq 0$.

Similarly, for the infected population:

$\frac{dI}{dt} = \beta SI + (1-\varepsilon)\beta VI - (\mu + \xi + \gamma + \delta)I$

At $I = 0$

$(\frac{dI}{dt})_{I=0} = 0$. Thus $I(t) \geq 0$ for all $t \geq 0$.

For the treated and the recovered compartments:

$\frac{dT}{dt} = \xi I - (\mu + \alpha)T$

At $T = 0$

$(\frac{dT}{dt})_{T=0} \geq 0$

Hence $T(t) \geq 0$ for all $t \geq 0$.

And

$\frac{dR}{dt} = \alpha T + \gamma I - (\mu + \gamma)R$

At $R(t) = 0$

$(\frac{dR}{dt})_{R=0} \geq \alpha T + \gamma I$

Hence $R(t) \geq 0$ for all $t \geq 0$

Thus, under non-negative initial conditions and biologically realistic parameter assumptions, all compartments remain non-negative for all $t \geq 0$.

3.1.2 INVARIANT REGION:

We show that all solutions of the system are bounded. The system (1) analysis will be analysed in the region Ω of the biological interest. Thus, we have the following theorem on the system (1) for boundedness property.

Theorem 3.2. The feasible region Ω defined by $\Omega = \{(S, I, V, T, R) \in R^5, S(t) \geq 0, I(t) \geq 0, V(t) \geq 0, T(t) \geq 0, R(t) \geq 0, 0 \leq N \leq Max\left\{N(0), \frac{\pi}{\mu}\right\}\}$, with initial condition, and $R(0) \geq 0$

is positively invariant and attracting with respect to system (1) for all $t \geq 0$, where $N = S + V + I + T + R$.

Proof: Here at time t, the total population is given by $N(t) = S(t) + V(t) + I(t) + T(t) + R(t)$. Therefore,

$\frac{dN}{dt} = \frac{dS}{dt} + \frac{dV}{dt} + \frac{dI}{dt} + \frac{dT}{dt} + \frac{dR}{dt}$.

Putting the values of system (1) in the above equation, we have:

$\frac{dN}{dt} = \pi - \mu S - \mu V - \mu I - \mu T - \mu R$,

$\frac{dN}{dt} = \pi - \mu N$.

Multiplying both sides by integrating factor $e^{\mu t}$, we get:

$$\int d(N.e^{\mu t}) = \int \pi.e^{\mu t}.dt + C, \text{ where } C \text{ is an integrating constant}$$

$$N.e^{\mu t} = \frac{\pi}{\mu}.\ e^{\mu t} + C.$$

Here, $N = N_0$ when $t = 0$.

Hence, $N \leq \frac{\pi}{\mu} + k.\ e^{-\mu t}$ where $k = \left(N_0 - \frac{\pi}{\mu}\right)$ which implies $0 \leq N(S, V, I, T, R) \leq \frac{\pi}{\mu}$.

4. Existence and Uniqueness of Solution for the SVITR Model

In this section, we develop the existence and uniqueness theorem for system (1), using the approach outlined by Syrti et al. [21]. We then provide proofs for the theorems.

Consider the general first order ordinary differential equation (ODE) of the form

$$\dot{x} = \emptyset(t, x), \emptyset(t^*) = x^* \qquad (3)$$

The following theorem helps us to determine the existence of the solution and moreover uniqueness of the solution corresponding to equation (3).

Theorem 4.1. (Uniqueness theorem): Let us consider the region $D = \{(t, x) |\ t \in N(t^*, \delta), x \in N(x^*, \varepsilon)\}$ with $x = \{x_i\}, i = 1,2,3, \dots, n$ and $x^* = \{x_i{}^*\}, i = 1,2,3, \dots, n$. The function $\emptyset(t, x)$ satisfied Lipschitz condition if $|\emptyset(t, x_1) - \emptyset(t, x_2)| \leq K|x_1 - x_2|$, when $(t, x_1) \in D, (t, x_2) \in D$ and $K \in R^+$, then there exists a solution of equation (1) in the domain D.

Remark 1. It is important to note the Lipschitz condition is satisfied by the requirement that $\frac{\delta \emptyset_i}{\delta x_j}$, $i, j = 1,2,3, \dots, n$ continuous and bounded in the region D.

Lemma 4.2. Let $\frac{\partial \emptyset_i}{\partial x_j}$, $i, j = 1,2,3, \dots, n$ is continuous and bounded on a closed convex domain D of R, then $\emptyset$ satisfies Lipschitz condition in D.

Theorem 4.3. let us consider the region $D = \{(t, x) |\, t \in N(t^*, \delta), x \in N(x^*, \varepsilon)\}$ with $x = \{x_i\}, i = 1,2,3, \dots, n$ and $x^* = \{x_i{}^*\}, i = 1,2,3, \dots, n$ such that $\frac{\delta \emptyset_i}{\delta x_j}$, $i, j = 1,2,3 \dots, n$ continuous and bounded in the region D. Then there exists a solution of the system (1) which is bounded in the region D.

Proof: let us consider the $\emptyset_i$, $i = 1,2,3,4,5$ as follows:

$$\emptyset_1 = \pi + \gamma R - \beta SI - (\phi + \mu)S \quad (4)$$

$$\emptyset_2 = \phi S - (1 - \varepsilon)\beta VI - \mu V \quad (5)$$

$$\emptyset_3 = \beta SI + (1 - \varepsilon)\beta VI - (\mu + \xi + \gamma + \delta)I \quad (6)$$

$$\emptyset_4 = \xi I - (\mu + \alpha) \quad (7)$$

$$\emptyset_5 = \alpha T - \gamma I - (\mu + \gamma)R \quad (8)$$

It is sufficient to show that $\frac{\partial \emptyset_i}{\partial x_j}$, $i, j = 1,2,3, \dots, n$ are continuous and bounded.

From equation (4) we have

$$\left|\frac{\partial \emptyset_1}{\partial S}\right| = |-\beta I - (\phi - \mu)| < \infty ,$$

$$\left|\frac{\partial \emptyset_1}{\partial V}\right| = |0| < \infty,$$

$$\left|\frac{\partial \emptyset_1}{\partial I}\right| = |-\beta S| < \infty,$$

$$\left|\frac{\partial \emptyset_1}{\partial T}\right| = 0 < \infty,$$

$$\left|\frac{\partial \emptyset_1}{\partial R}\right| = |\gamma| < \infty .$$

From equation (5) we have

$$\left|\frac{\partial \emptyset_2}{\partial S}\right| = |\phi| < \infty ,$$

$$\left|\frac{\partial \emptyset_2}{\partial V}\right| = |-\omega - (1-\varepsilon)\beta I - \mu| < \infty,$$

$$\left|\frac{\partial \emptyset_2}{\partial I}\right| = |-(1-\varepsilon)\beta V| < \infty,$$

$$\left|\frac{\partial \emptyset_2}{\partial T}\right| = 0 < \infty,$$

$$\left|\frac{\partial \emptyset_2}{\partial R}\right| = 0 < \infty .$$

From equation (6) we have

$$\left|\frac{\partial \emptyset_3}{\partial S}\right| = |\beta I| < \infty ,$$

$$\left|\frac{\partial \emptyset_3}{\partial V}\right| = |(1-\varepsilon)\beta I| < \infty,$$

$$\left|\frac{\partial \emptyset_3}{\partial I}\right| = |(1-\varepsilon)\beta V - \delta T - (\mu + \xi)| < \infty,$$

$$\left|\frac{\partial \emptyset_3}{\partial T}\right| = |-\delta I| < \infty,$$

$$\left|\frac{\partial \emptyset_3}{\partial R}\right| = 0 < \infty .$$

From equation (7) we have

$$\left|\frac{\partial \emptyset_4}{\partial S}\right| = 0 < \infty ,$$

$$\left|\frac{\partial \emptyset_4}{\partial V}\right| = 0 < \infty,$$

$$\left|\frac{\partial \emptyset_4}{\partial I}\right| = |\delta T| < \infty,$$

$$\left|\frac{\partial \emptyset_4}{\partial T}\right| = |-(\mu + \alpha)| < \infty,$$

$$\left|\frac{\partial \emptyset_4}{\partial R}\right| = 0 < \infty .$$

From equation (8) we have

$\left|\frac{\partial \emptyset_5}{\partial S}\right| = 0 < \infty$,

$\left|\frac{\partial \emptyset_5}{\partial V}\right| = 0 < \infty,$

$\left|\frac{\partial \emptyset_5}{\partial I}\right| = |\xi| < \infty,$

$\left|\frac{\partial \emptyset_5}{\partial T}\right| = |\alpha| < \infty,$

$\left|\frac{\partial \emptyset_5}{\partial R}\right| = |(\mu + \xi)| < \infty$.

We have clearly established that all those partial derivatives are continuous and bounded in D. Hence, there exist a unique solution in the region D.

5. EQUILIBRIUM POINT

For finding equilibrium points, we get the right-hand side of the system (1) equals to zero as follows:

$$\left.\begin{array}{c} \pi + \gamma R - \beta SI - \phi S - \mu S = 0 \\ \phi S - \varepsilon\beta VI - \mu V = 0 \\ \beta SI + \varepsilon\beta VI - (\mu + \xi + \gamma + \delta)I = 0 \\ \xi I - (\mu + \alpha)T = 0 \\ \alpha T - \gamma I - (\mu + \gamma)R = 0 \end{array}\right\} \quad (9)$$

On solving the above equations, then three equilibrium points in the coordinate $(S^*, V^*, I^*, T^*, R^*)$ are obtained and given as follows:

(i) Disease Free Equilibrium (DFE) point $E_0 = (S^0, V^0, I^0, T^0, R^0)$ $\left(\frac{\pi}{(\phi+\mu)}, \frac{\phi\pi}{\mu(\phi+\mu)}, 0,0,0\right)$.

(ii) Disease Endemic Equilibrium (DEE) point E_1 which is given as follows:

$$E_1 = (S^*, V^*, I^*, T^*, R^*)$$

Where $S^* = \frac{K}{\beta}\frac{\varepsilon\beta I^* + \mu}{D(I^*)}$

$I^* =$ Apositive real root of $a_2 I^2 + a_1 I + I_0 = 0$

$$V^* = \frac{\phi S^*}{(\varepsilon\beta I^* + \mu)}$$

$$T^* = C_T I^*$$

$$R^* = C_R I^*$$

Where $K = (\mu + \xi + \gamma + \delta)$

$$C_T = \frac{\xi}{(\mu + \alpha)}$$

$$C_R = \frac{\xi}{(\mu + \alpha)(\mu + \gamma)} + \frac{\gamma}{(\mu + \gamma)}$$

$$D_0 = \mu + \varepsilon\phi$$

$$D(I) = (\varepsilon\beta I^* + D_0)$$

$$a_2 = \varepsilon\beta(\gamma C_R - K)$$

$$a_1 = \pi\varepsilon\beta + \gamma C_R D_0 - K\mu - K\varepsilon(\varepsilon\beta I^* + \mu)$$

$$a_0 = \pi D_0 - \frac{K\mu(\mu + \phi)}{\beta}$$

6. BASIC REPRODUCTION NUMBER

Theorem 6.1 The basic reproduction number (R_0) of the model equation (1) is $\frac{\beta\pi}{(\mu+\xi+\gamma+\delta)(\phi+\mu)}\ (1 + \frac{(1-\varepsilon)\phi}{\mu})$

Proof:

To find the basic reproduction number R_0, we will be using the next- generation matrix method. The matrices F and V which represents the new infection terms and remaining transfer terms respectively are computed for the system of equations (1) as follows:

$$\frac{dI}{dt} = \beta SI + \varepsilon\beta VI - (\mu + \xi + \gamma + \delta)I$$

As per the New Generation Matrix Method, we get:

$$F = \beta SI + \varepsilon\beta VI \text{ and } V = (\mu + \xi + \gamma + \delta)I.$$

Then, the Jacobian of F and V at the disease-free equilibrium point $E_0 = (S_0, V_0, I_0, T_0, R_0) = \left(\frac{\pi}{(\phi+\mu)}, \frac{\phi\pi}{\mu(\phi+\mu)}, 0,0,0\right)$ is given by:

$F_I = \beta S_0 + \varepsilon\beta V_0$ and $V_I = (\mu + \xi + \gamma + \delta)$

Hence,

$$R_0 = \frac{F_I}{V_I} = \frac{\beta S_0 + \varepsilon\beta V_0}{(\mu + \xi + \gamma + \delta)}$$

Now at the DFE $E_0 = (S_0, V_0, I_0, T_0, R_0)\left(\frac{\pi}{(\phi+\mu)}, \frac{\phi\pi}{\mu(\phi+\mu)}, 0,0,0\right)$.

$$R_0 = \frac{\beta\pi}{(\mu + \xi + \gamma + \delta)(\phi + \mu)} \ (1 + \frac{(1-\varepsilon)\phi}{\mu})$$

7. Stability Analysis

When analyzing the stability of a dynamic system, it is important to investigate the Jacobian matrix J to comprehend how the system behaves close to a point of equilibrium. The Jacobian matrix gives a linear estimate of the system near that point, showing how tiny changes in the state variables S, V, I, T and R influence one another. Therefore, in order to perform a stability analysis on the system, we investigate the Jacobian matrix J at the equilibrium point. The matrix J representing the system is the Jacobian matrix and is given as follows:

$$J = \begin{pmatrix} J_{11} & 0 & -\beta S & 0 & \Upsilon \\ \phi & J_{22} & -\varepsilon\beta V & 0 & 0 \\ \beta I & \epsilon\beta I & J_{33} & 0 & 0 \\ 0 & 0 & \xi & J_{44} & 0 \\ 0 & 0 & \gamma & \alpha & J_{55} \end{pmatrix}$$

Where, $J_{11} = -(\phi + \mu) - \beta I$

$J_{22} = -(1-\varepsilon)\beta I - \mu$

$J_{33} = \beta S + (1-\varepsilon)\beta V - (\gamma + \xi + \delta + \mu)$

$J_{44} = -(\alpha + \mu)$

$J_{55} = -(\gamma + \mu)$

8. Local Stability at Disease-Free and Endemic Equilibrium Point

Theorem 8.1. Disease free equilibrium will be asymptotically stable if $R_0 < 1$.

Proof: The Jacobian of the system (1) at E_0 is given by

$$J_{E_0} = \begin{pmatrix} -(\phi+\mu) & 0 & -\beta S_0 & 0 & \Upsilon \\ \phi & -\mu & 0 & 0 & 0 \\ 0 & 0 & \beta S_0 + (1-\varepsilon)\beta V_0 - (\gamma + \xi + \delta + \mu) & 0 & 0 \\ 0 & 0 & 0 & -(\mu+\alpha) & 0 \\ 0 & 0 & \xi & -\alpha & -(\mu+\Upsilon) \end{pmatrix}.$$

Then, the eigen value of the J_{E_0} are:

$\lambda_1 = -(\mu + \xi)$,

$\lambda_2 = -\mu$

$\lambda_3 = \beta S_0 + (1-\varepsilon)\beta V_0 - (\gamma + \xi + \delta + \mu)$

$\lambda_4 = -(\mu + \alpha)$

$\lambda_2 = -(\mu + \Upsilon)$

Now λ_3 will be stable if $\lambda_3 < 0$

Which implies that $\beta S_0 + (1-\varepsilon)\beta V_0 - (\gamma + \xi + \delta + \mu) < 0$.

i.e., $R_0 = \frac{\beta S_0 + (1-\varepsilon)\beta V_0}{(\gamma + \xi + \delta + \mu)} < 1$

Hence the theorem.

Theorem 8.2. The endemic equilibrium points $\boldsymbol{E}^* = (\boldsymbol{S}^*, \boldsymbol{V}^*, \boldsymbol{I}^*, \boldsymbol{T}^*, \boldsymbol{R}^*)$ of the SVITR model is locally asymptotically stable if the real parts of all eigenvalues of the Jacobian matrix evaluated at $\boldsymbol{E}^*$are negative.

Proof: To investigate the local stability of the endemic equilibrium E^*,we evaluate the Jacobian matrix J of the system at E^*. Then the jacobian at E^*

$$J(E^*) = \begin{pmatrix} -(\phi + \mu) - \beta I^* & 0 & -\beta S^* & 0 & \Upsilon \\ \phi & -(1-\varepsilon)\beta I^* - \mu & -(1-\varepsilon)\beta V^* & 0 & 0 \\ \beta I^* & (1-\varepsilon)\beta I^* & \beta S^* + (1-\varepsilon)\beta V^* - (\gamma + \xi + \delta + \mu) & 0 & 0 \\ 0 & 0 & \xi & -(\alpha + \mu) & 0 \\ 0 & 0 & \gamma & \alpha & -(\gamma + \mu) \end{pmatrix}$$

We compute the characteristics equation of $J(E^*)$ is

$$|J(E^*) - \lambda I| = 0$$

This yields a fifth-degree polynomial in λ:

$$\lambda^5 + a_1\lambda^4 + a_2\lambda^3 + a_3\lambda^2 + a_4\lambda + a_5 = 0$$

According to the Routh–Hurwitz criterion, all roots of the above polynomial has negative real parts (i.e., $E^*$is locally asymptotically stable) if and only if all the Hurwitz determinants are positive. If this condition is satisfied, then E^* is locally asymptotically stable.

9. GLOBAL STABILITY ANALYSIS

Theorem 9.1. Disease-free equilibrium is global stability asymptotically stable if $R_0 < 1$.

Proof: Choosing a Lyapunov function involving infected and treated component $E(I,T) = I + T$.

$$\text{As } I(t) = \begin{cases} +ve & , t > 0 \\ 0 & , t = 0 \end{cases} \text{ and}$$

$$T(t) = \begin{cases} +ve & , t > 0 \\ 0 & , t = 0 \end{cases}$$

then $E(I,T)$ is positive definite and

$$\frac{dE}{dt} = \frac{dI}{dt} + \frac{dT}{dt}$$

$$\frac{dE}{dt} = \beta SI + \varepsilon\beta VI - \gamma I - \mu I - \xi I - \delta I + \xi I + \delta I - \mu T - \alpha T$$

$$\frac{dE}{dt} = I(\beta S + \varepsilon\beta V - \mu - \xi) - (\mu + \alpha)T$$

Now at the disease-free equilibrium point $E_0 = (S_0, V_0, I, T_0, R_0)\left(\frac{\pi}{(\phi+\mu)}, \frac{\phi\pi}{\mu(\phi+\mu)}, 0,0,0\right)$

Then

$$\frac{dE}{dt} = I(\beta S_0 + \varepsilon\beta V_0 - \mu - \xi) - (\mu + \alpha)T$$

From the theorem (8.1) , we get that $R_0 = \frac{\beta S_0 + \varepsilon\beta V_0}{(\gamma+\xi+\delta+\mu)}$

$$(\gamma + \xi + \delta + \mu)R_0 = (\beta S_0 + \varepsilon\beta V_0)$$

Then $\frac{dE(I,T)}{dt} = I\{R_0(\gamma + \xi + \delta + \mu) - \mu - \xi\} - (\mu + \alpha)T$

Now $\frac{dE}{dt} < 0$ if $I > 0$, $T \geq 0$ and $R_0 < 1$

Hence, disease- free equilibrium will be global stability asymptotically stable if $R_0 < 1$.

Theorem 9.2. The endemic equilibrium point $E^* = (S^*, V^*, I^*, T^*, R^*)$ of the SVITR model is globally asymptotically stable in the feasible region Ω $\{ 0 \leq \Omega \leq \frac{\pi}{\mu}\}$, provided $R_0 > 1$ and certain conditions on parameters hold.

Proof: Choosing a simple Lyapunov function involving infected and treated component

$$E = (S - S^*) - S\log\left(\frac{S}{S^*}\right) + (V - V^*) - V^*\log\left(\frac{V}{V^*}\right) + (I - I^*) - I^*\log\left(\frac{I}{I^*}\right) + (T - T^*) -$$

$$T^*\log\left(\frac{T}{T^*}\right) + (R - R^*) - R^*\log\left(\frac{R}{R^*}\right) \ .$$

This Lyapunov function is non-negative for all $(S, V, I, T, R) \in \Omega$ and $E = 0$ if and only if $(S, V, I, T, R) = (S^*, V^*, I^*, T^*, R^*)$.

Differentiating E along the trajectories of system (1), we obtain

$$\frac{dE}{dt} = \left(1 - \frac{S^*}{S}\right)\frac{dS}{dt} + \left(1 - \frac{V^*}{V}\right)\frac{dV}{dt} + \left(1 - \frac{I^*}{I}\right)\frac{dI}{dt} + \left(1 - \frac{T^*}{T}\right)\frac{dT}{dt} + + \left(1 - \frac{R^*}{R}\right)\frac{dR}{dt}$$

Substituting the values of the derivatives from SVITR model. then we have

$\frac{dE}{dt} \leq 0$ for all $t \geq 0$

With quantify if and only if $(S, V, I, T, R) = (S^*, V^*, I^*, T^*, R^*)$.

Hence, by LaSalle's Invariance Principle, the endemic equilibrium E^* is globally asymptotically stable in Ω.

10. SENSITIVITY ANALYSIS

To assess the relative impact of model parameters on the basic reproduction number (R_0), a normalized sensitivity analysis was performed. This analysis helps identify which parameters have the most influence on (R_0)thereby providing insights into the dynamics of disease transmission. Understanding the contribution of each parameter to $(R_0)$is crucial for effective intervention and control strategies. The normalized forward sensitivity index of (R_0) with respect to a given parameter X is defined as:

$$S_X^{R_0} = \frac{\delta R_0}{\delta X} * \frac{X}{R_0}$$

The sing of each index determines the level of importance of each parameter to the Basic Reproduction number. The positive value of the index determines the increasing nature and the negative value determines the decreasing nature of the importance of the basic reproduction number. This reveals how crucial the parameter is and how much it can be spread the disease. The call parameter-wise number

$$R_0 = \frac{\beta\pi}{(\mu + \xi + \gamma + \delta)(\phi + \mu)} \ (1 + \frac{(1 - \varepsilon)\phi}{\mu})$$

which is a parameter wise sensitivity index of the model can be found as follows:

For β :

$$S_{\beta}^{R_0} = \frac{\delta R_0}{\delta \beta} * \frac{\beta}{R_0} = 1$$

For π:

$$S_{\pi}^{R_0} = \frac{\delta R_0}{\delta\, \pi} * \frac{\pi}{R_0} = 1$$

For : ε

$$S_{\varepsilon}^{R_0} = \frac{\delta R_0}{\delta\, \varepsilon} * \frac{\varepsilon}{R_0} = \frac{-\varepsilon\, {\phi}/{\mu}}{(1 + \frac{(1-\varepsilon)\phi}{\mu})}$$

For ξ :

$$S_{\xi}^{R_0} = \frac{\delta R_0}{\delta\, \xi} * \frac{\xi}{R_0} = -\frac{\xi}{(\gamma + \xi + \delta + \mu)}$$

For δ :

$$S_{\delta}^{R_0} = \frac{\delta R_0}{\delta\, \delta} * \frac{\delta}{R_0} = -\frac{\delta}{(\gamma + \xi + \delta + \mu)}$$

For γ :

$$S_{\gamma}^{R_0} = \frac{\delta R_0}{\delta\, \gamma} * \frac{\gamma}{R_0} = -\frac{\gamma}{(\gamma + \xi + \delta + \mu)}$$

For ϕ :

$$S_{\phi}^{R_0} = \frac{\delta R_0}{\delta\, \phi} * \frac{\phi}{R_0} = -\frac{\phi}{\phi + \mu} + \frac{\varepsilon\, {\phi}/{\mu}}{\left(1 + \varepsilon\, {\phi}/{\mu}\right)}$$

For μ :

$$S_{\mu}^{R_0} = \frac{\delta R_0}{\delta \mu} * \frac{\mu}{R_0} = -\frac{\mu}{\phi + \mu} - \frac{\mu}{(\gamma + \xi + \delta + \mu)} - \frac{\varepsilon\, {\phi}/{\mu}}{\left(1 + \varepsilon\, {\phi}/{\mu}\right)}$$

Here we use $\beta = 1.2$, $\pi = 1000$, $\mu = 0.014$, $\xi = 0.01$, $\gamma = 0.2$, $\delta = 0.05$, $\phi = 0.01$, $\varepsilon = 0.5$ arbitrary numerical values to calculate sensitivity Index values

Table 2: Sensitivity Index and its value

Parameter	Sensitivity Index	Index value
β	1	1
π	1	1
ε	$\frac{-\varepsilon \phi/\mu}{(1+\frac{(1-\varepsilon)\phi}{\mu})}$	-0.263
ξ	$-\frac{\xi}{(\gamma+\xi+\delta+\mu)}$	-0.036
ϕ	$-\frac{\phi}{\phi+\mu}+\frac{\varepsilon \phi/\mu}{\left(1+\varepsilon \phi/\mu\right)}$	-0.154
γ	$-\frac{\gamma}{(\gamma+\xi+\delta+\mu)}$	-0.730
δ	$-\frac{\delta}{(\gamma+\xi+\delta+\mu)}$	-0.182
μ	$-\frac{\mu}{\phi+\mu}-\frac{\mu}{(\gamma+\xi+\delta+\mu)}-\frac{\varepsilon \phi/\mu}{\left(1+\varepsilon \phi/\mu\right)}$	-0.898

This table shows the contribution of each parameter of the basic reproduction number except for β and π which has a constant value 1 i.e., it is independent of any parameter. The sensitivity index $S_{\mu}^{R_0}, S_{\xi}^{R_0}, S_{\varepsilon}^{R_0}, S_{\phi}^{R_0}, S_{\gamma}^{R_0}$ are negative i.e., the value of R_0 decreases as the increases of $\mu, \xi, \varepsilon, \phi, \gamma$ The sensitivity index $S_{\beta}^{R_0}$ is constant i.e., any increases and decreases of β , the value of R_0 remain constant.

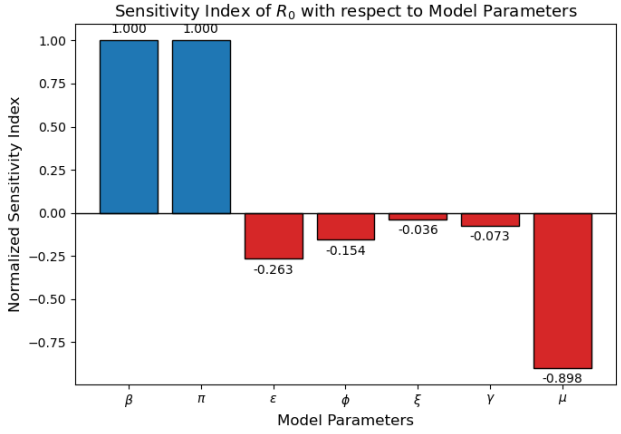

Figure 2: sensitivity index of R_0

11. NUMERICAL SIMULATION

In this section we study the dynamic behaviours of the system (1), MATLAB was used to simulate the system numerically. This system was evaluated under varying the value of the transmission rate (β), vaccination rate (ϕ) ,treatment rate (ξ) , vaccination efficacy(ε) , natural death rate μ . The simulation captured system behavior's both when $R_0 < 1$ and $R_0 > 1$ corresponding the stability at the disease-free equilibrium point (DFE) and the endemic equilibrium (EE) point.

For the first scenario (figure 3), parameter values are listed as $\beta = 0.14$,$\phi = 0.20$,$\varepsilon = 0.2$, $\alpha = 0.1$,$\gamma = 0.10 day^{-1}$,$\mu = 0.01\ day^{-1}$, $\pi = 0.01$ per day $\xi = 0.05$ per day,$\delta = 0.01$ per day .Under those condition, the basic reproduction number is

$$R_0 = \frac{\beta\pi}{(\mu + \xi + \gamma + \delta)(\phi + \mu)}\ (1 + \frac{(1-\varepsilon)\phi}{\mu})$$

$$R_0 < 1$$

The system exhibits rapid decay in both infected $I(t)$ and treated $T(t)$population, while the suspectable and the vaccinated individuals stabilize their initial populations. This indicated the global asymptotic stability of the population.

In the second scenario (figure 3), considered parameters values are $\beta = 0.25\ per\ day$,$\phi = 0.10$,$\varepsilon = 0.05$,$\alpha = 0.1$,$\gamma = 0.2$,$\mu = 0.01$, $\pi = 0.01$ $\xi = 0.1$,$\delta = 0.01$, which led to the basic reproduction number as,

$$R_0 = \frac{\beta\pi}{(\mu + \xi + \gamma + \delta)(\phi + \mu)}\ (1 + \frac{(1-\varepsilon)\phi}{\mu})$$

$$R_0 > 1$$

In this case, the infected and the treated population rise and stabilize at nonzero endemic levels, while the suspectable classes decrease and the recovered classes increase. the results confirm the local and global stability of the endemic equilibrium point, supporting the theorem (9.2) .

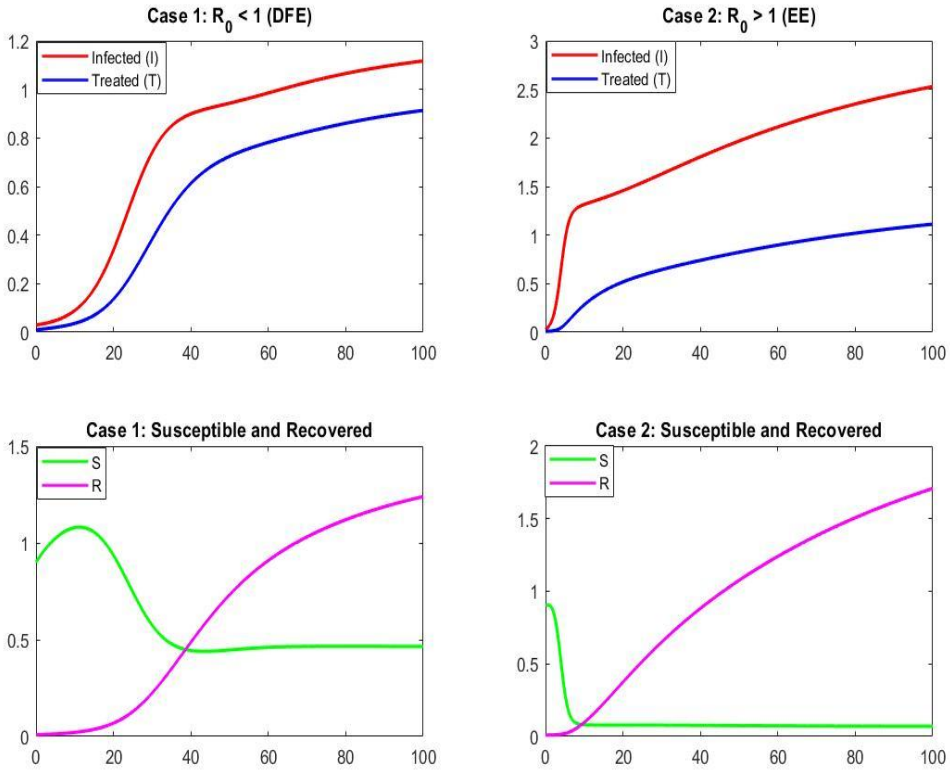

Figure 3: SVITR model Simulation on different R_0 Conditions

The normalized forward sensitivity index indicates reveals that the vaccination efficacy (ε) ,treatement rate (ξ) , and vaccination rate (ϕ) have strong negative negative values such as

$S_{\phi}^{R_0} = -0.154$

$S_{\varepsilon}^{R_0} = -0.263$

$S_{\xi}^{R_0} = -0.036$

This suggests that improving vaccination efficacy and increasing treatment initiation are the most effective interventions to reduce R_0 and control disease spread. conversely β remain positive and the constant sensitivity index, indicating its proportional contribution to transmission intensity.

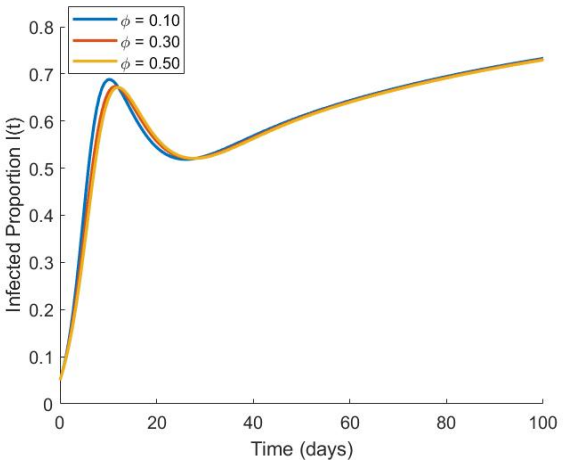

Figure 4: Growth of Influenza for different values of ϕ

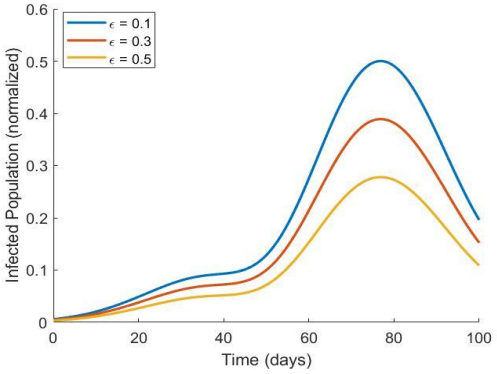

Figure 5: Growth of Influenza for different values of vaccination efficacy ε

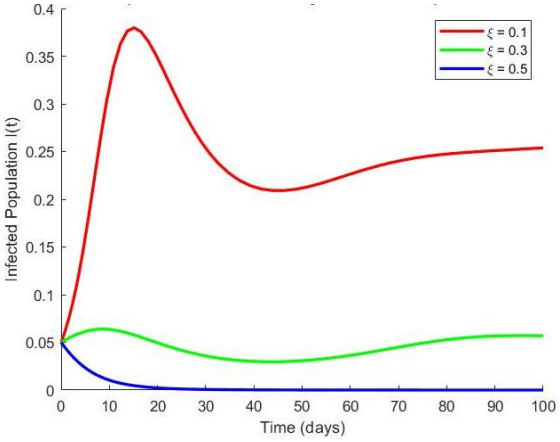

Figure 6: Growth of the infected population for different values of ξ

Figures 4-6 predict that as ϕ increases 0.01 to 0.1, the infected population peak reduces significantly confirming the role of mass vaccination in reducing incidence. As ε increases 0.1 to 0.5, lower the infection burden illustrating how the vaccination efficacy is important for reducing the disease effect. Enhanced treatment rate ξ causes the rapid decline in $I(t)$highlighting the early therapeutic persistence.

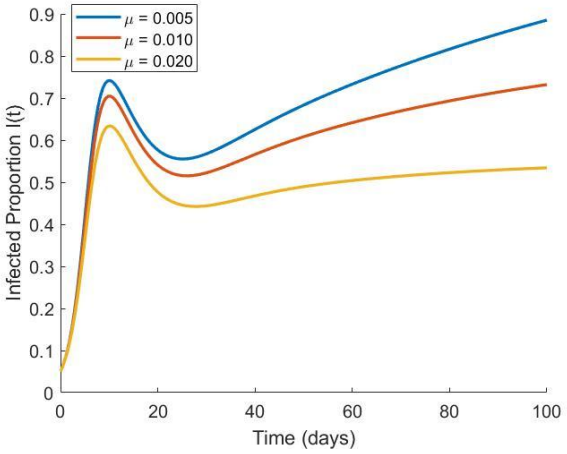

Figure 7: Growth of Influenza for different values of μ

Here natural death-rate μ increases 0.005 to 0.002, lower the infection burden illustrating how the natural death limits epidemic persistence.

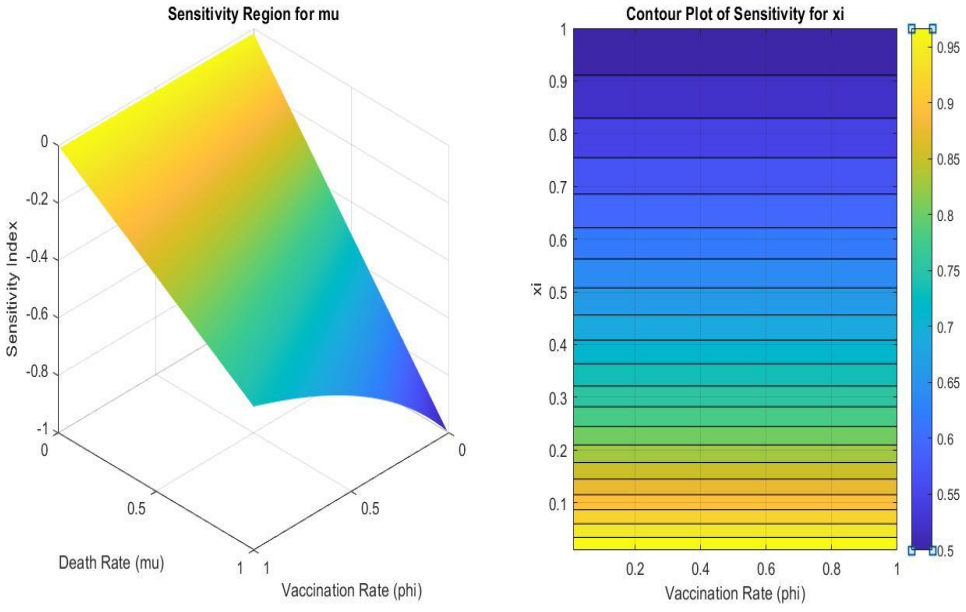

Figure 8: Region of the sensitivity index

In the figure (8) surface and the contour plots of the sensitivity index with respect to μ and ξ real-firm their importance in modifying R_0 .

12. BIFURCATION

Transcritical bifurcation occurs when $R_0 = 1$

$$i.e\frac{\beta S_0 + \varepsilon\beta V_0}{(\mu + \xi + \gamma + \delta)} = 1$$

$$or, \beta = \frac{(\mu + \xi + \gamma + \delta)}{S_0 + \varepsilon V_0}$$

$$\beta_{crit} = \frac{(\mu + \xi + \gamma + \delta)}{S_0 + \varepsilon V_0}$$

So, bifurcation parameter β is the critical values.

If $\beta < \beta_{crit} \rightarrow R_0 < 1$, then it stable, no infection occurs

If $\beta > \beta_{crit} \rightarrow R_0 > 1$, then above model becomes unstable, infection persists

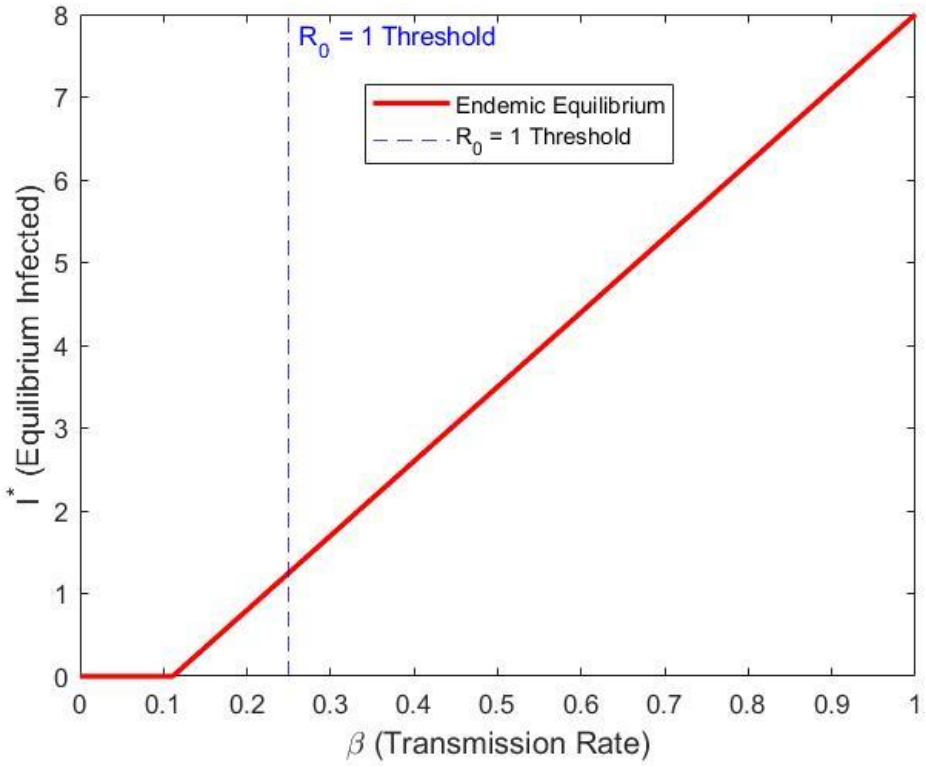

Figure 9: Transcritical Bifurcation diagram

Figure 9 predict that a forward transcritical bifurcation at the critical transmission rate β_c. For $\beta < \beta_c$ the disease-free equilibrium is globally stable and for $\beta > \beta_c$ the disease-free equilibrium loses stability, and the endemic equilibrium emerges.

Theorem12.1. The Transcritical bifurcation occurs when the transmission rate β passes through a critical value $\beta_{crit} = \frac{(\mu+\xi+\gamma+\delta)}{S_0+\varepsilon V_0}$.

Proof: From the model equation (1) we take only the infection component only

$$\frac{dI}{dt} = \beta SI + \varepsilon\beta VI - (\mu + \xi + \gamma + \delta)I$$

$$\frac{dT}{dt} = \xi I - (\mu + \alpha)T$$

Let us consider β be the infection parameters. Now we define $\beta = \beta_c + \mu$, where μ is very small. This will analyse the system for small perturbation $\mu \approx 0$ and small infection population $I, T \approx 0$.

Now for the disease-free equilibrium point $S = S_0, V = V_0, I = 0, T = 0, R = 0$

Then

$$\frac{dI}{dt} = (\beta S_0 + \varepsilon\beta V_0)I - (\mu + \xi + \gamma + \delta)I$$

$$\frac{dT}{dt} = \xi I - (\mu + \alpha)T$$

Now we consider, $m = (\mu + \xi + \gamma + \delta)$

And $n = (\mu + \alpha), \beta_c = \frac{\beta S_0+\varepsilon V_0}{m}$

Then,

$$\frac{dI}{dt} = [(S_0 + \varepsilon V_0)(\beta_c + \mu) - m]I$$

$$\frac{dT}{dt} = \xi I - nT$$

Putting the value of β_c , we have

$$\frac{dI}{dt} = [(S_0 + \varepsilon V_0)\mu I$$

$$\frac{dT}{dt} = \xi I - nT$$

Now we apply Center Manifold Theorem $\frac{dx}{dt} = Jx + f(x, \mu)$

Where J is the jacobian of thje matrix at $\mu = 0$ and f includes the nonlinear and higher order terms and $x = \begin{pmatrix} I \\ T \end{pmatrix}$.

At $\mu = 0$, the jacobian is $J = \begin{pmatrix} 0 & 0 \\ \xi & -n \end{pmatrix}$

The eigen values of the jacobian J is $\lambda_1 = 0, \lambda_2 = -n$. so, the system has a 1-dimensional center manifold (along I) and a stable manifold (along T).

Let $T = h(I, \mu)$ define center manifold near $I = 0, \mu = 0$ and substitute the system of the equation

$$\frac{dI}{dt} = [(S_0 + \varepsilon V_0)\mu I$$

This is a scalar ODE on the Center Manifold. We analyze the dynamics of the reduced equation:

$$\frac{dI}{dt} = \mu c I + higher\ order\ term$$

Where $c = (S_0 + \varepsilon V_0)$

This has a stable fixed point $I = 0, For\ \mu < 0\ (i.e\ \beta < \beta_c)$ and unstable fixed point $I = 0, For\ \mu > 0$.

Thus, the model undergoes the transcritical bifurcation for $\beta < \beta_c$

13. CONCLUSION

In this study, we developed and rigorously analyzed a nonlinear SVITR (Susceptible–Vaccinated–Infected–Treated–Recovered) model to explore the transmission dynamics of influenza and the impact of key epidemiological parameters. Through a combination of analytical techniques and numerical simulations, we demonstrated that both local and global stability of the disease-free and endemic equilibria are governed by the basic reproduction number R_0, which serves as a critical threshold parameter. The model confirms that the disease-free equilibrium is globally

asymptotically stable when $R_0 < 1$, while the endemic equilibrium becomes stable for $R_0 > 1$, a transition marked by a forward transcritical bifurcation.

Our sensitivity analysis identified vaccination efficacy, treatment rate, and vaccination rate as the most influential factors in controlling disease spread, offering actionable targets for public health intervention. In particular, the negative sensitivity indices associated with these parameters emphasize the effectiveness of improving vaccine performance and accelerating treatment initiation in reducing R_0. These findings align well with prior empirical and modelling studies, reinforcing the validity of our approach.

Numerical simulations further validated the theoretical results and revealed important dynamic behaviours under varying parameter scenarios. Notably, enhanced vaccination and treatment strategies significantly reduce peak infection levels and delay epidemic onset, highlighting the practical implications of parameter optimization.

Overall, this research provides a comprehensive framework for understanding influenza dynamics through mathematical modelling. The SVITR model presented here offers valuable insights for policymakers and epidemiologists seeking to develop robust, data-driven strategies for influenza mitigation. Future work may extend this framework to account for age structure, spatial heterogeneity, and co-infections with other respiratory pathogens, thereby enriching its applicability to real-world disease control efforts.

CONFLICT OF INTERESTS

The authors declare that there is no conflict of interests.

REFERENCE

[1] A.D. Iuliano, K.M. Roguski, H.H. Chang, D.J. Muscatello, R. Palekar, et al., Estimates of Global Seasonal Influenza-Associated Respiratory Mortality: A Modelling Study, Lancet 391 (2018), 1285-1300. https://doi.org/10.1016/s0140-6736(17)33293-2.

[2] Z. Wu, J.M. McGoogan, Characteristics of and Important Lessons from the Coronavirus Disease 2019 (COVID-19) Outbreak in China, JAMA 323 (2020), 1239-1242. https://doi.org/10.1001/jama.2020.2648.

[3] L. Lansbury, B. Lim, V. Baskaran, W.S. Lim, Co-Infections in People with COVID-19: A Systematic Review and Meta-Analysis, J. Infect. 81 (2020), 266-275. https://doi.org/10.1016/j.jinf.2020.05.046.

[4] C. Paules, K. Subbarao, Influenza, Lancet 390 (2017), 697-708. https://doi.org/10.1016/s0140-6736(17)30129-0.

[5] W.J. Guan, Z.Y. Ni, Y. Hu, W.H. Liang, C.Q. Ou, et al., Clinical Characteristics of Coronavirus Disease 2019 in China, New Engl. J. Med. 382 (2020), 1708-1720. https://doi.org/10.1056/nejmoa2002032.

[6] H. Yue, M. Zhang, L. Xing, K. Wang, X. Rao, et al., The Epidemiology and Clinical Characteristics of Co-infection of SARS-CoV-2 and Influenza Viruses in Patients during COVID-19 Outbreak, J. Med. Virol. 92 (2020), 2870-2873. https://doi.org/10.1002/jmv.26163.

[7] H.W. Hethcote, The Mathematics of Infectious Diseases, SIAM Rev. 42 (2000), 599-653. https://doi.org/10.1137/s0036144500371907.

[8] F. Brauer, C. Castillo-Chavez, Z. Feng, Mathematical Models in Epidemiology, Springer New York, 2019. https://doi.org/10.1007/978-1-4939-9828-9.

[9] A. Omame, N. Sene, I. Nometa, C.I. Nwakanma, E.U. Nwafor, et al., Analysis of COVID-19 and Comorbidity Co-infection Model with Optimal Control, Optim. Control. Appl. Methods 42 (2021), 1568-1590. https://doi.org/10.1002/oca.2748.

[10] M. Barik, C. Swarup, T. Singh, S. Habbi, et al., Dynamical Analysis, Optimal Control and Spatial Pattern in an Influenza Model with Adaptive Immunity in Two Stratified Population, AIMS Math. 7 (2022), 4898-4935. https://doi.org/10.3934/math.2022273.

[11] R.E. Hope-Simpson, The Role of Season in the Epidemiology of Influenza, J. Hyg. 86 (1981), 35-47. https://doi.org/10.1017/s0022172400068728.

[12] J. Lee, J. Kim, H.D. Kwon, Optimal Control of an Influenza Model with Seasonal Forcing and Age Structure, in: Proceedings of the Korean Society of Industrial and Applied Mathematics Conference, (2012).

[13] C.W. Kanyiri, K. Mark, L. Luboobi, Mathematical Analysis of Influenza A Dynamics in the Emergence of Drug Resistance, Comput. Math. Methods Med. 2018 (2018), 2434560. https://doi.org/10.1155/2018/2434560.

[14] T. Hussain, M. Ozair, K. Oare Okosun, M. Ishfaq, A. Ullah Awan, et al., Dynamics of Swine Influenza Model with Optimal Control, Adv. Differ. Equ. 2019 (2019), 508. https://doi.org/10.1186/s13662-019-2434-4.

[15] A. Moscona, Neuraminidase Inhibitors for Influenza, New Engl. J. Med. 353 (2005), 1363-1373. https://doi.org/10.1056/NEJMra050740.

[16] J. Wallinga, M. Lipsitch, How Generation Intervals Shape the Relationship Between Growth Rates and Reproductive Numbers, Proc. R. Soc. B: Biol. Sci. 274 (2006), 599-604. https://doi.org/10.1098/rspb.2006.3754.

[17] C. Fraser, Estimating Individual and Household Reproduction Numbers in an Emerging Epidemic, PLoS ONE 2 (2007), e758. https://doi.org/10.1371/journal.pone.0000758.

[18] D. Maji, A. Ghosh, Consequences of Parameters Mathematical Modelling of Two Interacting Viruses, in: Exploring Medical Statistics: Biostatistics, Clinical Trials, and Epidemiology, IGI Global, 2024: pp. 189-208. https://doi.org/10.4018/979-8-3693-2655-8.ch009.

[19] O. Diekmann, J.A.P. Heesterbeek, M.G. Roberts, The Construction of Next-Generation Matrices for Compartmental Epidemic Models, J. R. Soc. Interface 7 (2009), 873-885. https://doi.org/10.1098/rsif.2009.0386.

[20] J. Heffernan, R. Smith, L. Wahl, Perspectives on the Basic Reproductive Ratio, J. R. Soc. Interface 2 (2005), 281-293. https://doi.org/10.1098/rsif.2005.0042.

[21] B.M. Syrti, A. Devi, A.J. Kashyap, Analysis of Stability, Sensitivity Index and Hopf Bifurcation of Eco-Epidemiological SIR Model Under Pesticide Application, Commun. Biomath. Sci. 6 (2023), 126-144. https://doi.org/10.5614/cbms.2023.6.2.4.

[22] M.Y. Li, J.S. Muldowney, Global Stability for the SEIR Model in Epidemiology, Math. Biosci. 125 (1995), 155-164. https://doi.org/10.1016/0025-5564(95)92756-5.

[23] P. Das, R.K. Upadhyay, A.K. Misra, F.A. Rihan, P. Das, et al., Mathematical Model of COVID-19 with Comorbidity and Controlling Using Non-Pharmaceutical Interventions and Vaccination, Nonlinear Dyn. 106 (2021), 1213-1227. https://doi.org/10.1007/s11071-021-06517-w.

[24] K.M. Mohammad, A.A. Akhi, M. Kamrujjaman, Bifurcation Analysis of an Influenza A (H1N1) Model with Treatment and Vaccination, PLOS ONE 20 (2025), e0315280. https://doi.org/10.1371/journal.pone.0315280.

[25] M.E. Alexander, C. Bowman, S.M. Moghadas, R. Summers, A.B. Gumel, et al., A Vaccination Model for Transmission Dynamics of Influenza, SIAM J. Appl. Dyn. Syst. 3 (2004), 503-524. https://doi.org/10.1137/030600370.

[26] D. Maji, A. Ghosh, A Mathematical Modelling of Two Diseases: Influenza and SARS-COV-2, Linear Nonlinear Anal. 9 (2023), 221-229.